

# Negative linear compressibility in confined dilatating systems

E.V. Vakarin<sup>a</sup>, Yurko Duda<sup>b</sup>, J. P. Badiali<sup>a</sup>

<sup>a</sup> *UMR 7575 LECA ENSCP-UPMC, 11 rue P. et M. Curie, 75231 Cedex 05, Paris, France*

<sup>b</sup> *Programa de Ingeniería Molecular, Instituto Mexicano del Petróleo, 07730 D. F., México*

## Abstract

The role of a matrix response to a fluid insertion is analyzed in terms of a perturbation theory and Monte Carlo simulations applied to a hard sphere fluid in a slit of fluctuating density-dependent width. It is demonstrated that a coupling of the fluid-slit repulsion, spatial confinement and the matrix dilatation acts as an effective fluid-fluid attraction, inducing a pseudo-critical state with divergent linear compressibility and non-critical density fluctuations. An appropriate combination of the dilatation rate, fluid density and the slit size leads to the fluid states with negative linear compressibility. It is shown that the switching from positive to negative compressibility is accompanied by an abrupt change in the packing mechanism.

## I. INTRODUCTION

Compounds with a negative linear (or surface) compressibility have recently attracted an interest<sup>1-3</sup> because of their specific properties (stretch-induced densification and auxetic behavior), which might have promising applications. In the case of pure materials only "rare" crystal phases exhibit these effects, while for composite structures<sup>4</sup> it seems to be rather common. Recent experimental studies on insertion into organic<sup>5</sup> and non-organic<sup>6</sup> matrices reveal the negative compressibility effects due to the host-guest coupling. Conceptually similar escape transition<sup>7</sup> occurs when a polymer chain is compressed between

two pistons. Charge separation in confined fluids has also been accompanied<sup>8</sup> with the negative compressibility. These examples suggest that the insertion systems with confinement and swelling (dilatation) should exhibit this generic effect at appropriate conditions. In particular, two-particle systems confined to two-dimensional finite-size boxes of different geometry have been studied<sup>9–11</sup> in this context. It has been found that the isotherms exhibit a van der Waals-type (vdW) instability (loop) as the box size passes through a critical value. The instability has been associated with a prototype of a liquid-gas or a liquid-solid transition in many-body systems. A quite similar instability appears in two-dimensional granular media<sup>12</sup>, whose effective temperature decreases with the density, leading to a phase separation. Similar features have been detected<sup>13</sup> in hard discs confined to a narrow channel. Nevertheless, the non-monotonic behavior has been attributed to a sharp change in the accessible phase space, without any connection to collective effects typical for the conventional phase transitions. It is well-known, however, that a liquid-gas transition in finite systems<sup>14</sup> manifests itself through the negative compressibility states due to the surface effects.

Thus, it is quite interesting to find out if such a loop could exist in three-dimensional many-body systems and what is the physics behind. In particular, we focus on a prototype of an insertion system. One of the key features of such systems is a host dilatation (or contraction) upon a guest accommodation. This is evident from experiments with high-porosity materials, like aerogels<sup>15,16</sup>. Upon adsorption such matrices change in volume and their pore size distribution depends on the adsorbate pressure (or density). This effect is not exclusive to relatively soft gel-like matrices, it is quite common for carbon nanotubes<sup>17</sup> and various intercalation compounds<sup>18–20</sup>. In anisotropic cases (e.g. layered compounds) one deals with a competition of two effects. An increase of the lateral dimension (stretching) at constant number of particles tends to decrease the guest density. This usually induces a transversal shrink, leading to a densification in this direction. Since we have a composite host-guest system, the shrink does not obey the linear elasticity rules and, depending on the shrink intensity, one might expect the negative compressibility. In particular, it has been shown<sup>20</sup> that a nonlinear increase of the host size with the

guest concentration may induce a liquid-gas coexistence for the guest fluid even if the bulk liquid phase does not exist (e.g. a hard-sphere fluid). This means that the negative compressibility states were indeed present, but they were unstable under the conditions imposed.

Therefore, the objective of this paper is to find the conditions at which a coupling of the host dilatation and the guest confinement can stabilize the negative compressibility states. For this purpose we start with a quite simple model - the hard spheres, adsorbed in a softly-repulsing planar slit with a density-dependent width. The model contains all the relevant features: confinement, dilatation and spatial anisotropy. The latter is important because it offers a possibility of observing negative linear and positive tangential compressibilities, preserving the overall thermodynamic stability. On the other hand, in the absence of the dilatation (fixed slit width), the model is phenomenologically simple<sup>21,22</sup>. In particular, there is no a liquid-vapor transition (both in the bulk and in confined geometries). Such that the new aspects are not masked by the internal complexity. The system is analyzed by means of Monte Carlo (MC) simulation and a first-order perturbation theory<sup>23-25</sup>. Qualitative reliability of this approach has been tested in application to the liquid-vapor coexistence<sup>24</sup> and phase separation<sup>25</sup> in confined geometries.

## II. MODEL

Consider  $N$  hard spheres of diameter  $\sigma = 1$  in a planar slit with the surface area  $S$ . The slit itself is a part of a hosting system, whose coupling to the guest species changes the slit geometry. Therefore, the slit width  $h$  is not fixed, it fluctuates according to the fluid density (see below). For any  $h$  the total Hamiltonian is

$$H = H_{ff} + H_{fw}, \quad (1)$$

where  $H_{ff}$  is the hard sphere Hamiltonian,  $H_{fw}$  is the slit potential

$$H_{fw} = A \sum_{i=1}^N \left[ \frac{1}{z_i^k} + \frac{1}{(h - z_i)^k} \right]; \quad 1/2 \leq z_i \leq h - 1/2. \quad (2)$$

We do not take into account a short-ranged fluid-wall attraction, responsible for the surface adsorption or layering effects. The inverse-power shape for  $H_{fw}$  is chosen as a generic form of a soft repulsion, with  $k$  controlling the softness. For technical purposes we are working with  $k = 3$ . Moreover, our results are qualitatively insensitive to a particular choice of  $k$ .

It should be noted that we do not discuss an adsorption mechanism or the equilibrium between the pore and the bulk fluids. In our case  $N$  is fixed and we focus on the pressure variation due to the changes in the slit geometry.

### III. PERTURBATION THEORY

In practice the evolution of the matrix morphology is much slower than the fluid equilibration process. Then for a given width  $h$  we can calculate the fluid thermodynamics conditional to  $h$ .

#### A. Conditional equation of state and insertion isotherm

At any pore width  $h$  the free energy can be represented as

$$\beta F(h) = \beta F_0(h) - \ln \langle e^{-\beta H_{fw}} \rangle_0 \quad (3)$$

where  $F_0(h)$  is the free energy of a reference system, and  $\langle \dots \rangle_0$  is the average over the reference state. Taking a spatially confined hard sphere system (the one with  $A = 0$ ) as a reference, we consider a first order perturbation<sup>23–25</sup> for the conditional free energy

$$\beta F(h) = \beta F_0(h) + \beta S \rho(h) \int \prod_i dz_i H_{fw} \quad (4)$$

where  $\beta = 1/(kT)$  and  $\rho(h)$  is the pore density in the "slab" approximation

$$\rho(h) = \frac{N}{S(h-1)}, \quad (5)$$

ignoring a non-monotonic behavior of the density profile with increasing pore density. This is reasonable for wide pores and low fluid densities. The reference part is estimated

in the excluded volume approximation, while the perturbation contribution is  $N\Psi(h)$ , such that the total conditional free energy is

$$\beta F(h) = -N \ln \left[ \frac{1 - b\rho(h)}{\Lambda_T^3 \rho(h)} \right] - N + N\beta\Psi(h) \quad (6)$$

where  $b = 2\pi\sigma^3/3$  is the excluded volume factor,  $\Lambda_T$  is the thermal de Broglie length and

$$\Psi(h) = 16A \frac{h}{(1 - 2h)^2} \quad (7)$$

Tangential  $P_t(h)$  and normal  $P_n(h)$  pressures can be found as

$$P_t(h) = -\frac{1}{h-1} \left( \frac{\partial F(h)}{\partial S} \right)_{\beta, N}; \quad P_n(h) = -\frac{1}{S} \left( \frac{\partial F(h)}{\partial h} \right)_{\beta, N}. \quad (8)$$

This leads to

$$\beta P_t(h) = \frac{\rho(h)}{1 - b\rho(h)}; \quad \beta P_n(h) = \frac{\rho(h)}{1 - b\rho(h)} + 16A^* \frac{N}{S} \frac{2h + 1}{(2h - 1)^3}. \quad (9)$$

where  $A^* = \beta A$ . Equation (5) allows us to eliminate the surface density  $N/S$  in the favor of  $\rho(h)$  and we obtain the following equation of state

$$\beta P_n(h) = \frac{\rho(h)}{1 - b\rho(h)} + 16A^* \rho(h) \frac{(2h + 1)(h - 1)}{(2h - 1)^3} \quad (10)$$

Therefore, for a fixed  $h$ , our result is clear and simple. The tangential pressure has the bulk form, with the bulk density being replaced by the pore density. As a consequence of the first-order perturbative approach,  $P_t(h)$  does not depend on the slit-fluid interaction. As we will see later, the simulation results demonstrate that this dependence is indeed quite weak. If necessary this effect can be reproduced theoretically taking into account the second-order perturbation term. The normal pressure increases due to the repulsion  $A^*$  and decreases with increasing pore width  $h$ , such that  $P_n(h) = P_t(h)$  as  $h \rightarrow \infty$ .

Recall that we are dealing with a fixed  $N$ . The insertion process can be considered in the same framework. Just instead of the pressure components one would calculate the system response to increasing  $N$ – the insertion isotherm

$$\beta\mu(h) = \left( \frac{\partial \beta F(h)}{\partial N} \right)_{\beta, S, h} = \ln \left[ \frac{\Lambda_T^3 \rho(h)}{1 - b\rho(h)} \right] + \frac{b\rho(h)}{1 - b\rho(h)} + \beta\Psi(h) \quad (11)$$

which relates the fluid density and the chemical potential  $\mu(h)$ .

## B. Dilatation effect

As is discussed above, the pore dilatation can be taken into account, assuming that the width  $h$  is density-dependent. Real insertion materials are usually rather complex (multicomponent and heterogeneous). For that reason one usually deals with a distribution of pore sizes or with an average size. In this context we assume that  $h$  is known only statistically and the probability distribution  $f(h|\rho)$  is conditional<sup>26,27</sup> to the guest density  $\rho$ , which should be selfconsistently found from

$$\rho = \int dh f(h|\rho) \rho(h). \quad (12)$$

Then, taking our results for  $P_n(h)$  and  $P_t(h)$ , we can focus on the equation of state averaged over the width fluctuations.

$$P_i = \int dh f(h|\rho) P_i(h); \quad i = n, t. \quad (13)$$

This, however, requires a knowledge on the distribution  $f(h|\rho)$ . Even without resorting to a concrete form for  $f(h|\rho)$ , it is clear that the matrix reaction can be manifested as a change in the distribution width or/and the mean value. One of the simplest forms reflecting at least one of these features is a  $\delta$ -like distribution, ignoring a non-zero width.

$$f(h|\rho) = \delta[h - h(\rho)] \quad (14)$$

where  $\delta(x)$  is the Dirac  $\delta$ -function and the mean pore width  $h(\rho)$  is density-dependent.

$$h(\rho) = h_0(1 + \tanh[\Delta(\rho - \rho_0)] + \tanh[\Delta\rho_0]) \quad (15)$$

This form mimics a non-Vegard behavior, typical for layered intercalation compounds<sup>20</sup>. At low densities ( $\rho \ll \rho_0$ ) the dilatation is weak. The most intensive response is at  $\rho \approx \rho_0$ , and then the pore reaches a saturation, corresponding to its mechanical stability limit. Here  $\Delta$  is the matrix response constant or dilatation rate, controlling the slope near  $\rho \approx \rho_0$ .

From eq. (12) the average density is found to be

$$\rho = \frac{N}{S} \frac{1}{h(\rho) - 1} \quad (16)$$

Changing the surface density  $N/S$  we vary the average pore density  $\rho$ . This allows us to eliminate  $N/S$  in the favor of  $\rho$  in all thermodynamic functions. Combining eqs (10) and (13) we obtain

$$\beta P_n = \frac{\rho}{1 - b\rho} + 16A^* \rho \frac{(2h(\rho) + 1)(h(\rho) - 1)}{(2h(\rho) - 1)^3}; \quad (17)$$

It is convenient to introduce the compressibility function

$$\chi_n = \frac{1}{h(\rho) - 1} \frac{\partial h(\rho)}{\partial P_n} = \frac{1}{h(\rho) - 1} \frac{\partial h(\rho)}{\partial \rho} \frac{\partial \rho}{\partial P_n} \quad (18)$$

which vanishes in a non-swelling limit ( $h(\rho) = h_0$ ). It is clearly seen that  $\chi_n$  could be singular either if the swelling is discontinuous, or if  $P_n$  exhibits an inflection point. In what follows we focus on the second option.

In the case of a wide and weakly reacting pore we expand in terms of  $1/h_0$  and  $\Delta$ , obtaining a generic van der Waals form

$$\beta P_n = \frac{\rho}{1 - b\rho} + \frac{4A^*}{h_0} \rho - \frac{4A^* \Delta}{h_0} \rho^2 \quad (19)$$

Therefore, we have an interplay of several effects – the packing (first term), the fluid-matrix interaction (linear in density), and the matrix reaction (quadratic term). It is seen that a coupling of the fluid-slit repulsion ( $A$ ), spatial confinement ( $h_0$ ) and the matrix response ( $\Delta$ ) acts as an effective infinite-range fluid-fluid attraction (but just in one direction). Introducing a dimensionless temperature  $T^* = 1/(4A^*)$ , and solving

$$\frac{\partial P_n}{\partial \rho} = 0; \quad \frac{\partial^2 P_n}{\partial \rho^2} = 0 \quad (20)$$

we find the "critical" parameters

$$\rho_c = \frac{1}{3} \frac{\Delta + b}{\Delta b}; \quad T_c^* = \frac{1}{27} \frac{(2\Delta - b)^3}{bh_0 \Delta^2} \quad (21)$$

at which the normal compressibility  $\chi_n$  diverges. It is seen that a physically meaningful (with  $T_c^* > 0$ ) pseudo-criticality appears only at  $\Delta > b/2$ . In other words, the matrix

reaction  $\Delta$  should dominate the packing effects. In addition,  $T_c^*$  decreases with increasing pore width  $h_0$ .

It is well known that for bulk systems the vdW loop appearing at  $T^* < T_c^*$  is unphysical and one usually invokes the Maxwell construction, determining the liquid-vapor coexistence. As we will see below, in our case the loop is a physically justified effect. It appears as a competition between the packing, which tends to increase the pressure with increasing  $\rho$  and the slit dilatation, decreasing  $P_n$  with increasing  $\rho$ . As a result the states with negative linear compressibility are stabilized. Note that this behavior is not sensitive to the particular form (15) of  $h(\rho)$ . Moreover, the dilatation rate  $\Delta$  is essential, while the dilatation magnitude  $h(\rho) - h_0$  plays only a marginal role. As it should be, this effect disappears in the bulk limit  $h_0 \rightarrow \infty$  or in the case of insensitive matrices  $\Delta \rightarrow 0$ .

In order to be more accurate in comparison to the MC data the reference part is replaced by the Carnahan-Starling form

$$\beta P_n = \rho \frac{1 + \eta + \eta^2 - \eta^3}{[1 - \eta]^3} + 16A^* \rho \frac{(2h(\rho) + 1)(h(\rho) - 1)}{(2h(\rho) - 1)^3}; \quad \eta = \pi\rho/6. \quad (22)$$

This allows us to avoid the unphysical behavior at high densities.

#### IV. SIMULATION

In order to verify the existence of the loop predicted by the perturbation theory as well as to get more insight into the phenomenon the MC simulation of the model has been carried out. We applied the canonical NVT MC simulations of a confined hard sphere fluid to calculate the density profiles and pressure components. The simulation cell was parallelepiped in shape, with parallel walls at surface separation  $h$ , and surface area  $S = L_x \times L_y$ . The periodic boundary conditions were applied to the  $X$  and  $Y$  directions of the simulation box; the box length in the  $Z$  direction is fixed by the pore width. For a given pore width the adsorbed fluid density is chosen according to the Eq.(5). There was constant number of particles,  $N = 1000$ , and a desired fluid density has been get by adjusting the value of area,  $S$ . We repeated our simulation runs with bigger number



of particles,  $N = 1500$  and  $3000$ , but no significant differences were found. The density profiles,  $\rho(z)$ , were calculated in the usual way by counting the number of particles,  $N_i$  in the slabs of thickness  $d_z = 0.05$  parallel to the plane  $XY$  by using  $\rho(z) = N_i/v$ , where  $v$  is the slab volume  $v = d_z \times L_x \times L_y$ . The definition of Irving and Kirkwood<sup>28</sup> has been used to calculate the components of the pressure. The normal component of the pressure for the fluid-fluid interaction is

$$\beta P_n(z) = \rho(z) - \frac{\beta}{S} \left\langle \sum_i \sum_{j>i} \frac{dH_{ff}}{dr} \frac{z_{ij}^2}{|r_{ij}|} \Theta\left(\frac{z - z_i}{z_{ij}}\right) \Theta\left(\frac{z_j - z}{z_{ij}}\right) \right\rangle \quad (23)$$

where  $\rho(z)$  is the total density profile and  $\langle \dots \rangle$  denotes the average over the MC configurations. The tangential component,  $P_t(z)$ , has been calculated by substitution of  $z_{ij}^2$  by  $0.5(x_{ij}^2 + y_{ij}^2)$  in equation (23). For hard spheres the derivative of the potential is

$$\frac{d\beta H_{ff}}{dr} = -\delta(r - 1) \quad (24)$$

The Dirac  $\delta$  function in our simulation was approximated as

$$\delta(r - 1) = \frac{\Theta(r - 1) - \Theta(r - 1 - \Lambda)}{\Lambda}, \quad (25)$$

as  $\Lambda \rightarrow 0$ . In Eq. (25)  $\Lambda$  is used to define the region where two particles collides. A collision between particles occurs if  $1 < r < 1 + \Lambda$ . Therefore, for the particular case of hard spheres the averaged normal component of the pressure tensor for fluid-fluid interactions can be reduced to

$$\langle \beta P_n \rangle = \langle \rho \rangle + \frac{1}{V} \left\langle \sum_i \sum_{j>i} \frac{1}{\Lambda} \frac{z_{ij}^2}{|r_{ij}|} \Theta\left(\frac{z - z_i}{z_{ij}}\right) \Theta\left(\frac{z_j - z}{z_{ij}}\right) \right\rangle \quad (26)$$

The wall-fluid interaction is a function of  $z$  and affects only  $P_n$  while the tangential component remains the same. The normal pressure in this case is

$$\beta P_n^W(z) = \beta P_n^{W1}(z) + \beta P_n^{W2}(z) \quad (27)$$

where  $\beta P_n^{W1}(z)$  and  $\beta P_n^{W2}(z)$  are the fluid-wall contributions from surfaces located at  $z_{W1} = 0.5$  and  $z_{W2} = h - 0.5$ , respectively. These contributions are defined as

$$\beta P_n^{W1}(z) = -\frac{\beta}{S} \left\langle \sum_i \frac{dH_{fw}^i(z)}{dz} |z_i - z_{W1}| \Theta(z_i - z) \Theta(z - z_{W1}) \right\rangle \quad (28)$$

$$\beta P_n^{W2}(z) = -\frac{\beta}{S} \left\langle \sum_i \frac{dH_{fw}^i(z)}{dz} \Big|_{z_{W2} - z_i} \Theta(z_{W2} - z) \Theta(z - z_i) \right\rangle \quad (29)$$

These definitions of the pressure tensor treat the wall-particle interaction as a contribution to the intermolecular forces in a system consisting of the fluid and solid, rather than as an external field acting on the fluid. Thus the normal component of the pressure tensor must be independent of  $z$  as a condition of mechanical equilibrium and for a system containing bulk fluid must be equal to the pressure at the bulk density. Tangential components should approach the bulk pressure for sufficiently large  $h$ .

In this work we have taken parameter  $\Lambda$  equal to 0.001, 0.002, and 0.003 to make the extrapolation. The average normal component, includes the fluid-fluid and fluid-wall contributions given by equations (26) and (27). Each simulation runs  $5 \times 10^5$  MC cycles, with the first half for the system to reach equilibrium whereas the second half for evaluating the ensemble averages.

## V. RESULTS

In agreement with our theoretical prediction, the simulation results confirm that the negative compressibility states (the loop) appear only if the slit reaction  $\Delta$  reaches some threshold value  $\Delta^*$  which involves a combination of  $h_0$ ,  $\rho_0$  and  $A$ . The variation of the average density  $\rho$  due to the dilatation should dominate its variation, induced by the changes in the surface density  $N/S$ .

Pressure as a function of the average pore density is plotted in Figure 1. It is seen that the normal component  $P_n$  develops the loop with increasing pore-fluid repulsion  $A$ . The simulation results confirm that this feature is not an artefact of our theoretical approximations. As expected<sup>25</sup>, the perturbation theory systematically underestimates the magnitude of the fluid-wall repulsion,  $A$ , (overestimates the temperature  $T^*$ ) at which this effect takes place. The tangential component  $P_t$  is much less sensitive to the slit dilatation. This is coherent with our theoretical estimation. Interestingly, that  $P_t$  can be reasonably fitted by the expression for  $P_n$  taken at much lower  $A$  (see the insets).

Therefore, we expect that at sufficiently strong repulsion (low temperatures)  $P_t$  could also be non-monotonic. This would correspond to a fluid-solid transformation, which is not considered here. The loop becomes more pronounced with increasing dilatation rate  $\Delta$ . Since only one pressure component exhibits this behavior, there is no rational basis to suspect a vdW instability (of liquid-vapor type). Moreover, we are dealing with rather wide pores ( $h_0 = 10$ ) in order to avoid the narrow channel effects<sup>13</sup>. This makes us to search for an alternative explanation.

With this purpose we have analyzed the fluid structure at different densities. The density profiles are presented in Figure 2. It is obvious that the system does not exhibit strong density oscillations. It is worth noting, that our perturbation theory results are obtained in the 'slab' approximation, eq.(5), which does not take them into account. On the other hand, analysis of the density profiles indicates a sudden change of the packing regime in the negative compressibility region (in between the points  $A$  and  $B$ , marked in the Figure 1 (b)). The fluid film becomes more dilute with decreasing (e. g. due to a lateral stretching) density up to the point  $B$  with  $\rho = 0.32$ . This process goes uniformly in the middle of the film and at the periphery. Passing from  $\rho = 0.32$  to  $\rho = 0.29$  does not change the middle density, while the rarefaction takes place only near the slit walls. Upon reaching  $\rho = 0.25$  the film suddenly densifies in the middle. This corresponds to the inflection point in Figure 1 (b). Up to the point  $A$  with  $\rho = 0.2$  the film dilutes only at its periphery. Then we return to the usual uniform dilution with further decrease in the density. Therefore, there is a clear correlation between the negative compressibility states and the packing mechanism.

In order to study the redistribution of the fluid density we have calculated the average density  $\Gamma(z)$  in slabs of different thickness  $z$

$$\Gamma(z) = \int_0^z \rho(t) dt \quad (30)$$

The obtained results are presented in Figure 3. As seen,  $\Gamma(z)$  exhibits the same loop as the normal pressure does. Going towards the middle of the pore makes this effect more pronounced. Such similarity permits us to conclude that the fluid-wall soft repulsion

(coupled to the dilatation  $\Delta$ ) is a main reason of the fluid reordering inside the pore, and as a consequence the states with negative compressibility can occur. This is clearly seen from eq. (22), that gives a monotonic isotherm as  $A \rightarrow 0$  or  $\Delta \rightarrow 0$ .

It is interesting to mention that a similar trend has been described recently in the studies of mineral clays swelling<sup>30,31</sup>. Namely, Smith et al.<sup>31</sup> reported the simulation results of hydrated Na-smectites with variable layer charge. They found that the tendency to swell increases with increasing layer charge (increasing repulsion), which is consistent with our conclusions.

## VI. CONCLUSION

We have found that a coupling of the fluid-slit repulsion, spatial confinement and the slit dilatation acts as an anisotropic fluid-fluid attraction, inducing negative linear compressibility states. These states are shown to be related to an abrupt change in the packing regime, including a local densification in the middle with decreasing surface density. This resembles the stretch-densification effects<sup>1,2</sup> in negative compressibility materials. In the context of our model the mechanism is the following. Stretching in the lateral direction decreases the surface  $N/S$  and the pore  $\rho$  densities. This leads to a transversal shrink  $h(\rho)$  at the rate  $\Delta$ . This stabilizes the negative transversal compressibility when the rate passes some threshold value. This mechanism is quite different from that explored in the low-dimensional systems<sup>9-11,13</sup>, where the loops appeared essentially due to the small-size effects restricting the phase space accessibility when the box length became comparable with the particle size. As a result, the vdW feature is found<sup>11</sup> to be very sensitive to the box geometry (rectangular or spherical). In our case we deal with a three-dimensional system where the particles can exchange their positions almost freely ( $10 \leq h(\rho)/\sigma \leq 30$ ), although the phase space is somewhat restricted by the slit-fluid repulsion. Nevertheless, our model shares some of the low-dimensional features<sup>9-11,13</sup> and we recover the usual monotonic behavior in the bulk limit  $h_0 \rightarrow \infty$ .

Since the tangential pressure component does not exhibit this effect, the system does

not undergo a phase transition (at least in its traditional sense). This is confirmed by the absence of strong density fluctuations (in both directions). On the other hand, the loop appears in the direction, along which our system is finite (finite  $h$ ) and, therefore, the negative compressibility can be considered as a finite-size effect<sup>14</sup>, vanishing in the bulk limit. Nevertheless, an inclusion of an attractive fluid-fluid interaction would result<sup>23,24</sup> in the pore condensation. In this respect it would be quite interesting to analyze how the above stretch-densification coexists with the true critical behavior. The role of more isotropic geometries (e.g. spherical pores) as well as that of a non-zero distribution width ( $f(h|\rho)$ ) and the potential softness  $k$  could also be discussed. Another interesting point is to describe the sorption behavior, that is, changing  $\rho$  by varying  $N$  at fixed  $S$ . In this way we can mimic a "dosen" adsorption<sup>29</sup> or the equilibrium with an infinite bulk reservoir. We plan to analyze these issues in a future work.

## REFERENCES

- <sup>1</sup> R. H. Baughman, S. Stafstrom, C. Cui, S. O. Dantas, *Science* **279**, 1522 (1998)
- <sup>2</sup> R. H. Baughman, *Nature (London)* **425**, 667 (2003)
- <sup>3</sup> J. A. Kornblatt, *Science* **281**, 143a (1998)  
E. B. Sirota, H. E. King Jr., *Science* **281**, 143a (1998)  
R. H. Baughman, C. Cui, *Science* **281**, 143a (1998)
- <sup>4</sup> M. Bowick, A. Cacciuto, G. Thorleifsson, A. Travesset, *Phys. Rev. Lett.* **87**, 148103 (2001)
- <sup>5</sup> T. Goworek, J. Wawryszczuk, R. Zaleski, *Chem. Phys. Lett.* **402**, 367 (2005)  
A. M. Soto, B. I. Kankia, P. Dande, B. Gold, L. A. Marky, *Nucl. Acids Research* **29**, 3638 (2001)
- <sup>6</sup> C. A. Perotoni, J. A. H. da Jornada, *Phys. Rev. Lett.* **78**, 2991 (1997)
- <sup>7</sup> L. I. Klushin, A. M. Skvortsov, F. A. M. Leermakers, *Phys. Rev. E* **69**, 061101 (2004)
- <sup>8</sup> J. Yu, L. Degreve, M. Lozada-Cassou, *Phys. Rev. Lett.* **79**, 3656 (1997)
- <sup>9</sup> A. Awazu, *Phys. Rev. E* **63**, 032102 (2001)
- <sup>10</sup> T. Munakata, G. Hu, *Phys. Rev. E* **65**, 066104 (2002)
- <sup>11</sup> S. H. Suh, S. C. Kim, *Phys. Rev. E* **69**, 026111 (2004)
- <sup>12</sup> M. Argentina, M. G. Clerc, R. Soto, *Phys. Rev. Lett.* **89**, 044301 (2002)
- <sup>13</sup> Ch. Forster, D. Mukamel, H. A. Posch, *Phys. Rev. E* **69**, 066124 (2004)
- <sup>14</sup> F. Gulminelli, Ph. Chomaz, *Phys. Rev. Lett.* **82**, 1402 (1999)
- <sup>15</sup> G. W. Scherer, *Adv. Coll. Interface Sci.* **76-77**, 321 (1998)
- <sup>16</sup> P. Thibault, J. J. Prejean, L. Puech, *Phys. Rev. B* **52**, 17491 (1995)
- <sup>17</sup> M. Mercedes Calbi, F. Toigo, M. W. Cole, *Phys. Rev. Lett.* **86**, 5062 (2001)

- <sup>18</sup> E. V. Vakarin, J.P. Badiali, M. D. Levi, D. Aurbach, *Phys. Rev. B*, **63**, 014304 (2001)
- <sup>19</sup> E. V. Vakarin, J. P. Badiali, *J. Phys. Chem. B* **106**, 7721 (2002)
- <sup>20</sup> E. V. Vakarin, J. P. Badiali, *Solid State Ionics* **171**, 2004 (2004)
- <sup>21</sup> J. Wu, *AIChE J.* in press (2005).
- <sup>22</sup> J. Alejandro, M. Lozada-Cassou, L. Degreve, *Molec. Phys.* **88**, 1317 (1996).
- <sup>23</sup> M. Schoen, D. J. Diestler, *J. Chem. Phys.* **109**, 5596 (1998)
- <sup>24</sup> G. J. Zarragoicoechea, V. A. Kuz, *Phys. Rev. E* **65**, 02110 (2002)
- <sup>25</sup> Y. Duda, E. V. Vakarin, J. Alejandro, *J. Colloid. Interface. Sci.* **258**, 10 (2003)
- <sup>26</sup> E. V. Vakarin, J. P. Badiali, *Electrochim. Acta* **50**, 1719 (2005)
- <sup>27</sup> E. V. Vakarin, J. P. Badiali, *Surf. Sci.* **565**, 279 (2004)
- <sup>28</sup> J. H. Irving, J. G. Kirkwood, *J. Chem. Phys.* **18**, 817, (1950).
- <sup>29</sup> G. Amarasekera, M. J. Scarlett, D. E. Mainwaring, *J. Phys. Chem.* **100**, 7580 (1996)
- <sup>30</sup> G. Odriozola, J. F. Aguilar, *J. Chem. Phys.* **123**, 174708 (2005)
- <sup>31</sup> D. Smith, Y. Wang, H. D. Whitley, *Fluid Phase. Equilib.* **222**, 189 (2004)

## FIGURES

FIG. 1. Normal and tangential pressures (the insets) in the case of a weakly (a) and strongly (b) repulsive slit. The other parameters are  $h_0 = 10$ ,  $\Delta = 15$ ,  $\rho_0 = 0.3$

FIG. 2. MC density profiles at different densities (indicated). Other parameters as in the previous figure.

FIG. 3. Average fluid density in slabs of different thickness  $z$  (lines) and the normal pressure component (line with symbols).



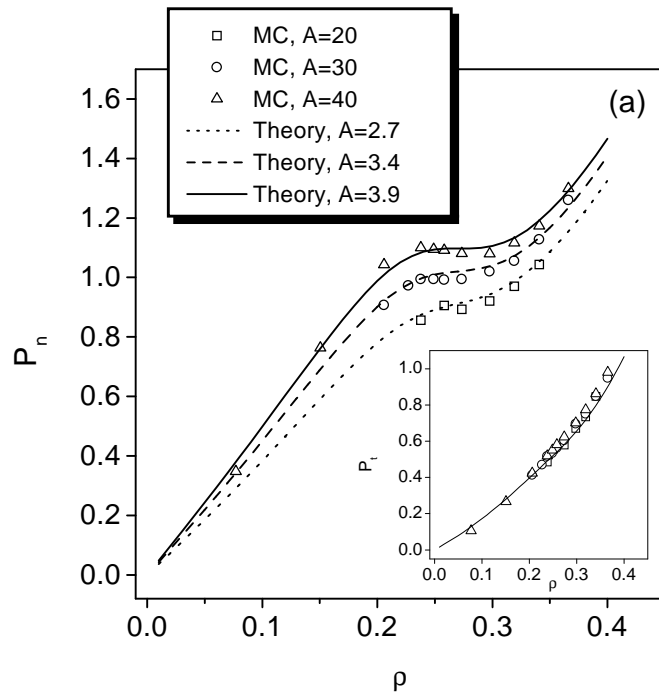


Figure 1(a)

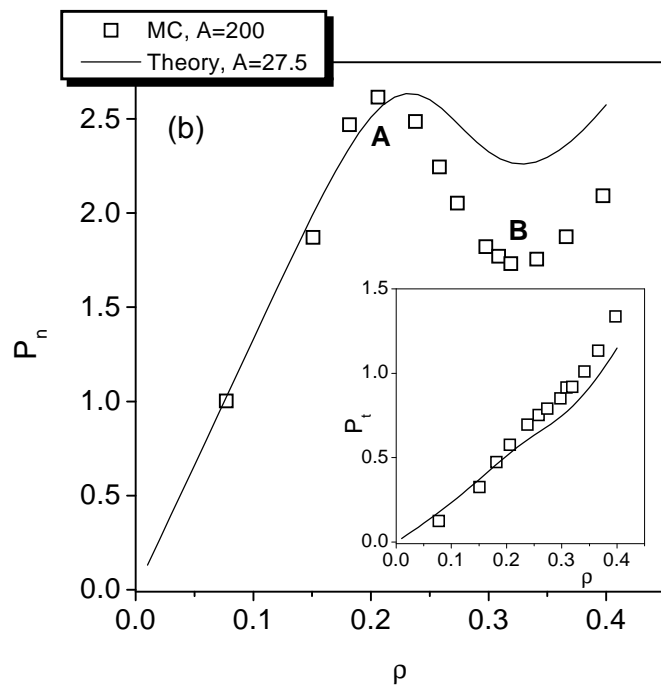


Figure1 (b)

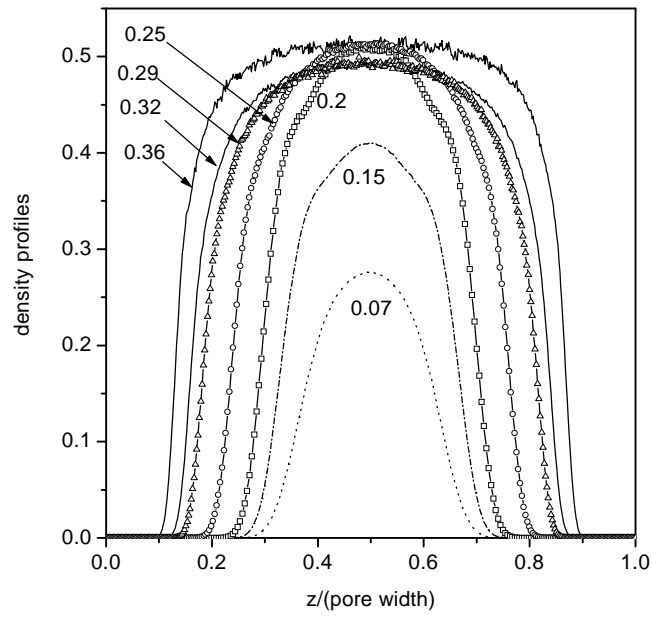


Figure 2

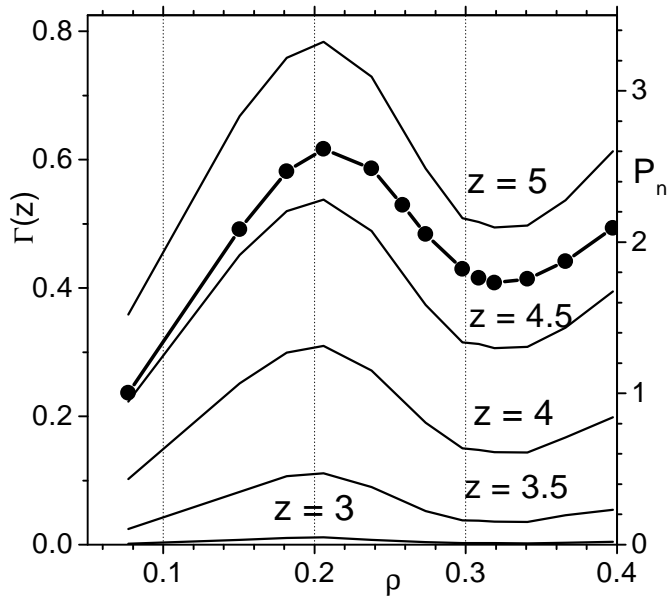


Figure 3